Commun. Comput. Phys.
doi: 10.4208/cicp.OA-2017-0013

Vol. **22**, No. 5, pp. 1333-1361
November 2017

Analysis of Geometrically Consistent Schemes with Finite Range Interaction

Hongliang Li[1] and Pingbing Ming[2,*]

[1] *Institute of Electronic Engineering, Microsystem and Terahertz Research Center, China Academy of Engineering Physics, Mianyang, 621900, China.*
[2] *The State Key Laboratory of Scientific and Engineering Computing, Academy of Mathematics and Systems Science, Chinese Academy of Sciences, No. 55, East Road Zhong-Guan-Cun, Beijing 100190, China and School of Mathematical Sciences, University of Chinese Academy of Sciences, Beijing 100049, China.*

Received 18 January 2017; Accepted (in revised version) 25 April 2017

Abstract. We analyze the geometrically consistent schemes proposed by E. Lu and Yang [6] for one-dimensional problem with finite range interaction. The existence of the reconstruction coefficients is proved, and optimal error estimate is derived under sharp stability condition. Numerical experiments are performed to confirm the theoretical results.

AMS subject classifications: 65N15, 65N30

Key words: Quasicontinuum method, atomic-to-continuum coupling, stability, finite range interactions.

1 Introduction

The main motivation for the multiscale coupling method is that the macroscale model is sufficiently accurate except the isolated regions in which the microscale model is required to resolve the details of the local events take place in these regions. The quasicontinuum (QC) method [31] is one of the earliest multiscale coupling method for modeling the mechanical deformation of crystalline solids. There are two class methods in QC: the energy-based method and the force-based method. In this paper we focus on the energy-based method, and refer to [16] and [14,15] for a review on the force-based method and its recent progress. We list several representatives of the energy-based QC method: the dead load force correction method [29]; the quasinonlocal method (QNL) [30] and the

*Corresponding author. *Email addresses:* lihongliang@mtrc.ac.cn (H. L. Li), mpb@lsec.cc.ac.cn (P. B. Ming)

generalized QNL [12, 27, 28]; the geometrically consistent scheme (GCS) [6] and its generalization [24, 25]; and the blended QC [1, 26, 32]. The essential difference among these methods are the strategies to deal with the energy of the atoms inside the atomistic-to-continuum (a/c) interface. It is worthwhile to mention that there are also some other a/c energy-based coupling methods such as the optimization-based coupling method [19].

In this study we shall focus on GCS proposed by E. Lu and Yang. This scheme depends only on the lattice structure of the system and works for all existing empirical potentials with an arbitrary interaction range. It generalizes QNL proposed in [30]. New variants of GCS have recently been proposed in [24, 25], which have been proven to be first-order consistent. A reflection method in the spirit of GCS was constructed in [21]. Though there seems no straightforward extension of this method to 2d/3d, the authors proved the first-order accuracy of the reflection method in 1d under sharp stability condition. A set of coefficients has to be precomputed in the implementation of GCS. Such coefficients (we call GCS coefficients) for various lattice structures with different interaction ranges have been charted in [6], while its existence for problems with arbitrary interaction range interaction remains unproved. Progress in this direction has been made in [24] in 2d. We prove the existence of GCS coefficients in 1d, and hope it may provide certain insights for 2d/3d.

Ming and Yang [17] analyzed GCS for an atomic chain with second neighboring interaction. Uniformly first-order accuracy has been proved in the discrete $W^{1,\infty}$ norm. However, the stability condition is suboptimal, and their analysis is confined to second neighboring interaction. This motivates our study on GCS for finite range interaction, which is particularly important when van der Waals type interactions play an essential role. For example, we are interested in modeling the mechanical interaction between atom clusters. We firstly prove that the GCS coefficients indeed exist for 1d chain with finite range interaction, while it is not unique. Next we derive a special symmetric solution, which essentially coincides with that in [6] for the interaction range less than five. Motivated by [24,25], we propose a minimizing algorithm to obtain new sets of GCS coefficients. Numerical evidence suggests that GCS with such coefficients may have smaller error. We establish an identity for GCS coefficients, upon which we prove the first-order consistency of GCS in a negative Sobolev norm. Using this identity, a discrete Wirtinger inequality and a generalized polarization identity, we prove that GCS with finite range interaction is stable under the sharp stability condition for Dirichlet boundary value problem. The stability condition is sharp in the sense that the difference between the stability condition of GCS and that of the atomic model is of $\mathcal{O}(\varepsilon^2)$, where ε is the lattice spacing. We test the accuracy of GCS by a set of numerical examples, which show that GCS has optimal convergence rate in the discrete $W^{1,p}$ norm for $2 \leq p \leq \infty$. The analysis is carried out for the pairwise potential for brevity, which can be extended for many-body potential by combining the techniques from [7] and [11, 16].

The paper is organized as follows. In Section 1, we introduce the setup of the problem and the geometrical consistent scheme. In Section 2, we propose a condition under which GCS coefficients exist. A special set of GCS coefficients is explicitly derived, and

a constrained minimizing algorithm is introduced to determine the GCS coefficients. In Section 3 and Section 4, we estimate the consistency error and prove the sharp stability of GCS. In Section 5, several numerical examples are reported, which confirms the optimal convergence rate of GCS with different ranges of interaction and different GCS coefficients.

1.1 Preliminary

Let $\varepsilon=1/N$ be the lattice spacing and we consider a chain that occupies $\Omega_\varepsilon=[-1,1]\cap\varepsilon\mathbb{Z}$. The reference state is denoted by $x=i\varepsilon$ for $i=-N,\cdots,N$, while the deformed state $y(x)=x+u(x)$ with displacement u that belongs to

$$\mathcal{U}_\varepsilon=\{u:\varepsilon\mathbb{Z}\to\mathbb{R}\,|\,u(x)=0,\ x\in\varepsilon\mathbb{Z}\setminus\Omega_\varepsilon\}.$$

For any $k\in\mathbb{Z}$, we define

$$\mathcal{U}_{\varepsilon,k}=\{u:\varepsilon\mathbb{Z}\to\mathbb{R}\,|\,u(x)=0,\ x\in\varepsilon\mathbb{Z}\setminus\Omega_{\varepsilon,k}\},$$

where $\Omega_{\varepsilon,k}=\{-(N+k)\varepsilon,\cdots,N\varepsilon\}$ and $\Omega_{\varepsilon,-k}=\{-N\varepsilon,\cdots,(N+k)\varepsilon\}$. The translation operator T is defined as $(Tu)(x)=u(x+\varepsilon)$. We define the discrete gradient operator as

$$D_k:\mathcal{U}_\varepsilon\to\mathcal{U}_{\varepsilon,k}\quad\text{with}\ \ D_k=\varepsilon^{-1}(T^k-I),$$

where I is the identity operator. We shall use the shorthand $Du=D_1u$ and $D_-u=D_{-1}u$. The average operator is defined as

$$A_k=\sum_{l=0}^{k-1}T^l\quad\text{and}\quad A_{-k}=\sum_{l=0}^{k-1}T^{-l},\qquad k\in\mathbb{N}.$$

The ℓ^2-inner product is defined for any $u,v\in\mathcal{U}_\varepsilon$ as

$$\langle u,v\rangle:=\sum_{x\in\Omega_\varepsilon}\varepsilon u(x)v(x),$$

the corresponding discrete weighted ℓ^p_ε-norm is defined as

$$\|v\|_{\ell^p_\varepsilon}:=\begin{cases}\left(\sum_{x\in\Omega_\varepsilon}\varepsilon|v(x)|^p\right)^{1/p}, & 1\le p<\infty,\\ \max\limits_{x\in\Omega_\varepsilon}|v(x)|, & p=\infty.\end{cases}$$

We shall use the following relations for any $u,v\in\mathcal{U}_\varepsilon$:

$$\langle u,D_kv\rangle=\langle A_{-k}u,Dv\rangle\quad\text{and}\quad\langle u,D_{-k}v\rangle=\langle A_ku,D_{-1}v\rangle,\tag{1.1}$$

and

$$\langle u,Dv\rangle=-\left\langle T^{-1}u,D_-v\right\rangle\quad\text{and}\quad\langle u,D_-v\rangle=-\langle Tu,Dv\rangle,\tag{1.2}$$

which may be easily verified by summation by parts.

1.2 Atomistic model and Cauchy-Born model

For any $r_{\rm cut}\in\mathbb{N}$, we assume that an atom interacting with at most $r_{\rm cut}$ neighboring atoms, and ϕ is a potential function satisfying [20]

1. $\phi\in C^3((0,\infty);\mathbb{R})$;
2. there exists r^*, such that ϕ is convex in $(0,r^*)$ and concave in $(r^*,+\infty)$.

It is clear that the Lennard-Jones potential [10] satisfies the above assumptions. We further assume that

$$Dy(x)>r^*/2 \quad \text{for all } \ x\in\Omega_{\varepsilon,1}. \tag{1.3}$$

The site energy of the atom x is

$$S_{\rm a}(x)=\frac{\varepsilon}{2}\sum_{k=1}^{r_{\rm cut}}\big(\phi(D_k y(x))+\phi(-D_{-k}y(x))\big). \tag{1.4}$$

The total energy is defined for any $y-x\in\mathcal{U}_\varepsilon$ as

$$E_{\rm a}^{\rm tot}(y)=E_{\rm a}(y)-\langle f,y\rangle \quad \text{with } \ E_{\rm a}(y)=\sum_{x\in\Omega_\varepsilon}S_{\rm a}(x).$$

The atomistic model problem is: Find $y_{\rm a}-x\in\mathcal{U}_\varepsilon$ such that

$$y_{\rm a}\in\operatorname{argmin}E_{\rm a}^{\rm tot}(y), \tag{1.5}$$

where the argmin denotes the set of the local minima of $E_{\rm a}^{\rm tot}(y)$. The Euler-Lagrange equation associated with (1.5) is

$$\langle\delta E_{\rm a}[y_{\rm a}],v\rangle=\langle f,v\rangle, \quad \forall v\in\mathcal{U}_\varepsilon,$$

where $\delta E_{\rm a}[y]$ is the Fréchet derivative of $E_{\rm a}$.

The total energy of the Cauchy-Born (CB) [2] elastic model can be written as

$$E_{\rm c}^{\rm tot}(y)=\sum_{x\in\Omega_\varepsilon}\varepsilon\sum_{k=1}^{r_{\rm cut}}\phi\big(kDy(x)\big)-\langle f,y\rangle.$$

We aim to find $y_{\rm c}-x\in\mathcal{U}_\varepsilon$ such that

$$y_{\rm c}\in\operatorname{argmin}E_{\rm c}^{\rm tot}(y).$$

The site energy of the atom x can be defined as

$$S_{\rm c}(x)=\frac{\varepsilon}{2}\sum_{k=1}^{r_{\rm cut}}(\phi(kDy(x))+\phi(-kD_{-1}y(x))). \tag{1.6}$$

1.3 Geometrically consistent schemes

In QC method, the atomistic model is coupled with the CB elastic model. It is well-known that a straightforward coupling method suffers from ghost forces [29], which may cause $\mathcal{O}(1)$ error in strain. We refer to [5, §8] for a nice summary on the influence of ghost forces and refer to [4, 17] for more details.

To remove the ghost force, a buffer layer $\Omega_{\mathrm{a/c}}$ between the atomistic region Ω_{a} and the continuum region Ω_{c} is introduced in both QNL (quasinonlocal) and GCS (geometrically consistent scheme), and the site energies for the atoms inside the buffer layer have to be carefully defined. The site energy of atom x depends on the relative distance between x and atoms inside the interaction range, i.e., both $D_k y(x)$ and $kD_1 y(x)$ are used to reconstruct the relative distance between atom x and atom $x+k\varepsilon$. It is natural to introduce a general discrete gradient operator

$$\mathcal{D}_k : \mathcal{U}_\varepsilon \to \mathcal{U}_{\varepsilon,k}$$

for any $k \in \{\pm 1, \cdots, \pm r_{\mathrm{cut}}\}$. Similar to the representations (1.4) and (1.6), the site energy is defined as

$$S_{\mathrm{a/c}}(x) = \frac{\varepsilon}{2} \sum_{k=1}^{r_{\mathrm{cut}}} \left[\phi(\mathcal{D}_k y(x)) + \phi(-\mathcal{D}_{-k} y(x)) \right].$$

For QNL, and for any $x \in \Omega_{\mathrm{a/c}}$,

$$\mathcal{D}_{\pm k} y(x) := \begin{cases} D_{\pm k} y(x), & x \pm k\varepsilon \in \Omega_a, \\ kD_{\pm 1} y(x), & \text{otherwise.} \end{cases}$$

QNL uses the positions of the nearest neighbor atoms to reconstruct the relative positions of other atoms. Therefore, QNL is limited to the case that the interaction only involves the second nearest neighbors.

The operator $\mathcal{D}_{\pm k}$ in GCS is defined as a linear combination of $D_{\pm k}$ and $kD_{\pm 1}$:

$$\mathcal{D}_{\pm k} y(x) := C_{\pm k}(x) D_{\pm k} y(x) + (1 - C_{\pm k}(x)) k D_{\pm 1} y(x), \tag{1.7}$$

where the coefficient $C_{\pm k}(x)$ varies for different k and atom site x. It is convenient to require that $C_{\pm k}(x) = 0$ for $x \in \Omega_{\mathrm{a}}$, and $C_{\pm k}(x) = 1$ for $x \in \Omega_{\mathrm{c}}$. We shall use the shorthand $\mathcal{D}_{\pm k} y$ for $\mathcal{D}_{\pm k}[y](x)$ when there is no confusion occurs.

The total energy is defined as

$$E^{\mathrm{tot}}_{\mathrm{gcs}}(y) = E_{\mathrm{gcs}}(y) - \langle f, y \rangle \quad \text{with} \quad E_{\mathrm{gcs}}(y) = \sum_{x \in \Omega_\varepsilon} S_{\mathrm{a/c}}(x). \tag{1.8}$$

Now we find $y_{\mathrm{gcs}} - x \in \mathcal{U}_\varepsilon$ such that

$$y_{\mathrm{gcs}} \in \operatorname{argmin} E^{\mathrm{tot}}_{\mathrm{gcs}}(y). \tag{1.9}$$

To remove the influence of ghost force, we need to impose

$$\delta E_{\rm gcs}[y]\big|_{y=y_F}=0, \tag{1.10}$$

where $y_F=Fx$ for any $F>0$. A direct calculation yields

$$\partial_{y(x)}\big(\langle \mathcal{D}_k y,1\rangle+\langle -\mathcal{D}_{-k}y,1\rangle\big)\big|_{y=y_F}=0,\quad k=1,\cdots,r_{\rm cut},\quad \forall x\in\Omega_\varepsilon. \tag{1.11}$$

This condition is equivalent to [6, Definition 3], which depends only on the lattice structure of the crystal, while is independent of the interaction potentials. For the system with many-body interaction, the same condition (1.11) can be deduced from (1.10).

Remark 1.1. GCS has been extended to high dimension problem in [6]. One may derive identities similar to (1.7) and (1.10), which are expected to play essential role in the analysis and implementation of GCS as we shall shown later on for 1d chain. However, a rigorous study of GCS for high dimension problem is largely an open problem.

2 Existence of the GCS coefficients

In this part, we seek conditions under which (1.11) is valid, and find practical ways to determine the coefficients.

Substituting (1.7) into (1.11), we obtain, for any $1\le k\le r_{\rm cut}$,

$$C_k(x-k\varepsilon)-kC_k(x-\varepsilon)+(k-1)C_k(x)=(k-1)C_{-k}(x)-kC_{-k}(x+\varepsilon)+C_{-k}(x+k\varepsilon). \tag{2.1}$$

This condition is trivial for $k=1$. For any $2\le k\le r_{\rm cut}$, we assume that the thickness of the buffer layer is M_k, and we write

$$\Omega_{\rm a}=\{x=i\varepsilon\mid i=-N,\cdots,0\},$$
$$\Omega_{\rm a/c}=\{x=i\varepsilon\mid i=1,\cdots,M_k\},$$

and

$$\Omega_{\rm c}=\{x=i\varepsilon\mid i=M_k+1,\cdots,N\}.$$

It is clear that for any $2\le k\le r_{\rm cut}$,

$$C_{\pm k}(x)\equiv 1,\quad x<\varepsilon,\quad \text{and}\quad C_{\pm k}(x)\equiv 0,\quad x>M_k\varepsilon. \tag{2.2}$$

Let $x=(M_k+k)\varepsilon$ in (2.1), we obtain $C_k(x)=0$ for $x=M_k\varepsilon$. Next, letting $x=(M_k+k-1)\varepsilon$ in (2.1), and using the above fact, we obtain $C_k(x)=0$ for $x=(M_k-1)\varepsilon$. By the principle of induction, we have $C_k(x)=0$ for $x\ge(M_k-k+1)\varepsilon$. Applying the same procedure to $x=\{(-k+1)\varepsilon,\cdots,-\varepsilon\}$, we obtain $C_{-k}(x)=1$ for $x\le k\varepsilon$. Therefore,

$$C_k(x)=\begin{cases}0, & x>(M_k-k)\varepsilon,\\ 1, & x<\varepsilon,\end{cases}\quad\text{and}\quad C_{-k}(x)=\begin{cases}0, & x>M_k\varepsilon,\\ 1, & x<(k+1)\varepsilon.\end{cases} \tag{2.3}$$

It remains to determine $C_k(x)$ for $x=\varepsilon,\cdots,(M_k-k)\varepsilon$ and $C_{-k}(x)$ for $x=(k+1)\varepsilon,\cdots,M_k\varepsilon$.

By the above condition, we get $M_k\geq k$, i.e., the thickness of $\Omega_{a/c}$ is at least k. When $k=2$, the thickness $M_k=2$ is just the one used in QNL [30]. When $k\geq 3$, ghost forces cannot be removed if $M_k=k$.

By (2.3), the condition (2.1) is valid for $x\in\Omega_a\cup\Omega_c$. Denote

$$\eta=[C_k(\varepsilon),\cdots,C_k((M_k-k)\varepsilon),C_{-k}((k+1)\varepsilon),\cdots,C_{-k}(M_k\varepsilon)]^T.$$

We write

$$A\eta=\zeta, \tag{2.4}$$

where $A=[A_1,-A_2]$ with $A_1,A_2\in\mathbb{R}^{M_k\times(M_k-k)}$, and

$$A_1(i,j)=\begin{cases} k-1, & i-j=0,\\ -k, & i-j=1,\\ 1, & i-j=k,\\ 0, & \text{otherwise,}\end{cases} \quad\text{and}\quad A_2(i,j)=\begin{cases} 1, & i-j=0,\\ -k, & i-j=k-1,\\ k-1, & i-j=k,\\ 0, & \text{otherwise,}\end{cases} \tag{2.5}$$

and $\zeta\in\mathbb{R}^{M_k}$ with

$$\zeta=[\overbrace{k-2,-2,\cdots,-2,k-2}^{k},0,\cdots,0]^T.$$

Our main result in this section is

Theorem 2.1. *For $2\leq k\leq r_{cut}$, Problem* (2.4) *is solvable when $M_k\geq 2k-2$.*

If $M_k=2k-2$, Problem (2.4) *has a unique solution*

$$\begin{cases} C_k(x)=1-\dfrac{x(x+\varepsilon)}{k\varepsilon(k-1)\varepsilon}, & \varepsilon\leq x\leq(k-2)\varepsilon,\\ C_{-k}(x)=\dfrac{(x-2k\varepsilon)(x+\varepsilon-2k\varepsilon)}{k\varepsilon(k-1)\varepsilon}, & (k+1)\varepsilon\leq x\leq(2k-2)\varepsilon.\end{cases} \tag{2.6}$$

Proof. First, we prove (2.4) has a solution (2.6) when $M_k=2k-2$.

By the kth equation of (2.4), we find $\eta_{k-1}=1-2/k$, this proves the second equation of (2.6) with $x=(k+1)\varepsilon$. Next we solve the first equation of (2.4) to obtain

$$\eta_1=1-2/[k(k-1)],$$

which verifies the first equation of (2.6) with $x=\varepsilon$. Now we assume that the first equation of (2.6) is true for $x\leq i\varepsilon$, and the second equation of (2.6) is true for $x\leq(k+i)\varepsilon$, then we solve the $(k+i)$th equation of (2.4)

$$\eta_i+(1-k)\eta_{k+i-2}+k\eta_{k+i-1}=0,$$

and obtain

$$\eta_{k+i-1}=\frac{1}{k}\left(\frac{(k-i)(k-i-1)}{k}-1+\frac{i(i+1)}{k(k-1)}\right)=\frac{(k-i-1)(k-i-2)}{k(k-1)},$$

which verifies the second equation of (2.6) with $x=(k+i+1)\varepsilon$.

Next we solve the $(i+1)$th equation of (2.4)

$$-k\eta_i+(k-1)\eta_{i+1}-\eta_{k+i-1}=-2,$$

and obtain

$$\eta_{i+1}=1-(i+1)(i+2)/[k(k-1)],$$

which verifies the first equation of (2.6) with $x=(i+1)\varepsilon$. By the principle of induction, we prove identity (2.6) for all x.

Second, we prove (2.4) has a unique solution when M_k=2k−2. Selecting the 2,⋯,(2k−3)th row vectors of A, we get a submatrix $\widehat{A}\in\mathbb{R}^{(2k-4)\times(2k-4)}$ with

$$\widehat{A}=\begin{bmatrix}-kI+(k-1)P & -P\\ P^{\mathrm{T}} & kI-(k-1)P^{\mathrm{T}}\end{bmatrix},$$

where I is the $k-2$ by $k-2$ identity matrix, and $P\in\mathbb{R}^{(k-2)\times(k-2)}$ is a Toeplitz matrix defined by $P\equiv(a_{i-j})_{i,j=1}^{k-2}$ with $a_1=1$ and $a_i=0$ otherwise. Since

$$\begin{aligned}&\widehat{A}\begin{bmatrix}I & (k-1)I\\ 0 & I\end{bmatrix}\begin{bmatrix}I & 0\\ -k^{-1}P^{\mathrm{T}} & I\end{bmatrix}\\ =&\begin{bmatrix}-kI+(k-1)(P+P^{\mathrm{T}})-(k-2)PP^{\mathrm{T}} & k[(k-2)P-(k-1)I]\\ 0 & kI\end{bmatrix},\end{aligned}$$

then

$$\det\widehat{A}=\det(kI)\det(-kI+(k-1)(P+P^{\mathrm{T}})-(k-2)PP^{\mathrm{T}}).$$

A straightforward calculation gives

$$\det(-kI+(k-1)(P+P^{\mathrm{T}})-(k-2)PP^{\mathrm{T}})=(-1)^{k-2}(k-1)^{k-3}(2k-3).$$

This implies

$$\det\widehat{A}=(-k)^{k-2}(k-1)^{k-3}(2k-3)\neq0.$$

We conclude that rank(A)=2k−4. Therefore, the linear system (2.4) has a unique solution of the form (2.6).

If $M_k<2k-2$, we have the kth row vector of A is a zero vector, while the right-hand side equals to $k-2$ by (2.4). This is absurd. Therefore, we conclude that the ghost forces cannot be removed when $M_k<2k-2$.

Denote the ith column of A as b_i. If $M_k>2k-2$, then we obtain $\{b_1,\cdots,b_{k-2}\}\cup\{b_{M_k-k+1},\cdots,b_{M_k-2}\}\cup\{\zeta\}$ are linearly dependent by (2.6). Therefore, rank(A)=rank(A,ζ). This proves that Problem (2.4) is solvable. □

Remark 2.1. If we switch the role of Ω_a and Ω_c, then the coefficients change to

$$\begin{cases} C_k(x)=\dfrac{x(x+\varepsilon)}{k\varepsilon(k-1)\varepsilon}, & \varepsilon\le x\le(k-2)\varepsilon, \\ C_{-k}(x)=1-\dfrac{(x-2k\varepsilon)(x-2k\varepsilon+\varepsilon)}{k\varepsilon(k-1)\varepsilon}, & (k+1)\varepsilon\le x\le(2k-2)\varepsilon. \end{cases} \tag{2.7}$$

When $M_k>2k-2$, we may elongate the solution for $M_k=2k-2$ by setting the remaining components by zeroes. Although the thickness of the buffer layer M_k are defined separately for different interaction range k, we shall use a common thickness of the buffer layer $M=M_{r_{cut}}$ in practice.

Remark 2.2. The authors in [6] pointed out that GCS reconstruction coefficient equations (1.11) are solvable for 1d chain and the solution is not unique. They listed the solution for $r_{\text{cut}}=1,\cdots,5$, which coincides with (2.6).

Due to the non-uniqueness of the reconstruction coefficients, we find a solution by solving the following ℓ^p-minimization problem as

$$\eta^*=\text{argmin}\|\eta\|_{\ell^p} \quad \text{subject to } A\eta=\zeta, \tag{2.8}$$

where $p=1$ and 2 in this work. It is natural to seek for the ℓ^1-minimizer, because it corresponds to the most sparse solution of the system, which may reduce the cost in the implementation. The ℓ^2-minimizer is used for comparison's sake. The numerical effect of such reconstruction coefficients will be reported in the last section. We note that similar ideas have been used in [24, 25] to determine the coefficients of the coupling method. Their motivation comes from the special structure of the consistency error.

As an example, we set $k=5$ and $M_5=9$, the ℓ^1-minimizer and ℓ^2-minimizer are reported in Table 1. Additional information for the coefficients can be found in Table 4 to Table 7 in the Appendix.

It is clear that some coefficients in Table 1 are negative, which may lead to undesirable numerical instability. To avoid such instability, we impose an extra positiveness constraint on the minimization problem (2.8) as

$$\eta^*=\text{argmin}\|\eta\|_{\ell^p} \quad \text{subject to } A\eta=\zeta, \quad 0\le\eta\le 1. \tag{2.9}$$

The positive ℓ^1-minimizer can be found in Table 2 and Table 3, which is almost the same with (2.6) provided that we set the coefficients with the same magnitude of $\mathcal{O}(10^{-9})$ as

Table 1: The ℓ^1 and ℓ^2 optimal GCS coefficients.

	$C_5(\varepsilon)$	$C_5(2\varepsilon)$	$C_5(3\varepsilon)$	$C_5(4\varepsilon)$	$C_{-5}(6\varepsilon)$	$C_{-5}(7\varepsilon)$	$C_{-5}(8\varepsilon)$	$C_{-5}(9\varepsilon)$
ℓ^1	0.7847	0.4694	0.0541	-0.4612	0.1388	-0.0459	-0.1306	-0.1153
ℓ^2	0.7833	0.4667	0.0500	-0.4667	0.1333	-0.0500	-0.1333	-0.1167

Table 2: The positive ℓ^1 optimal GCS coefficients $C_k(x)$.

	ε	2ε	3ε	4ε	5ε	6ε	7ε	8ε	9ε
$C_2(x)$	0	0	0	0	0	0	0	0	0
$C_3(x)$	0.6667	0	0	0	0	0	0	0	0
$C_4(x)$	0.8333	0.5000	0	0	0	0	0	0	0
$C_5(x)$	0.9000	0.7000	0.4000	0	0	0	0	0	0

Table 3: The positive ℓ^1 optimal GCS coefficients $C_{-k}(x)$.

	ε	2ε	3ε	4ε	5ε	6ε	7ε	8ε	9ε
$C_{-2}(x)$	1	1	0	0	0	0	0	0	0
$C_{-3}(x)$	1	1	1	0.3333	0	0	0	0	0
$C_{-4}(x)$	1	1	1	1	0.5000	0.1667	0	0	0
$C_{-5}(x)$	1	1	1	1	1	0.6000	0.3000	0.1000	0

zero. We move the results for the positive ℓ^2-minimizer to Table 8 and Table 9 in the Appendix.

The next lemma concerns an identity for the reconstruction coefficients.

Lemma 2.1. *For any $k=1,\cdots,r_{cut}$ and $x\in\Omega_\varepsilon$, there holds*

$$(kI-A_{-k})C_k(x)+T(kI-A_k)C_{-k}(x)=0. \tag{2.10}$$

The above identity can be written into

$$k\big(C_k(x)+C_{-k}(x+\varepsilon)\big)=\sum_{i=1}^{k}\big(C_k(x-i\varepsilon+\varepsilon)+C_{-k}(x+i\varepsilon)\big).$$

Let $k=2$ in the above equation, we obtain

$$C_2(x)+C_{-2}(x+\varepsilon)=C_2(x-\varepsilon)+C_{-2}(x+2\varepsilon),$$

which can be rewritten into

$$C_2(x)-C_{-2}(x+2\varepsilon)=C_2(x-\varepsilon)-C_{-2}(x+\varepsilon),$$

which immediately implies $C_2(x)=C_{-2}(x+2\varepsilon)$. This is just [17, Lemma 5.7], which has been extensively exploited in [17] to analyze GCS with k=2. Lemma 2.1 is a natural extension of this result to finite range interaction, which shall play a key role in the subsequent analysis.

Proof. For any $x\in\Omega_\varepsilon$, we denote

$$F(x):=(kI-A_{-k})C_k(x)+T(kI-A_k)C_{-k}(x).$$

It is clear that $F(x)=0$ for either $x\in\Omega_{\rm a}$ or $x\in\Omega_{\rm c}$.

For any fixed integer $k\in\mathbb{N}$, we sum identity (2.1) to obtain

$$\begin{aligned}&\sum_{i=0}^{k-1}\big(C_k(x-i\varepsilon-k\varepsilon)-kC_k(x-i\varepsilon-\varepsilon)+(k-1)C_k(x-i\varepsilon)\big)\\=&\sum_{i=0}^{k-1}\big(C_{-k}(x-i\varepsilon+k\varepsilon)-kC_{-k}(x-i\varepsilon+\varepsilon)+(k-1)C_{-k}(x-i\varepsilon)\big).\end{aligned}\tag{2.11}$$

By telescope sum trick, the left-hand side of the above identity can be written into

$$\begin{aligned}&\sum_{i=0}^{k-1}\big(C_k(x-i\varepsilon-k\varepsilon)-kC_k(x-i\varepsilon-\varepsilon)+(k-1)C_k(x-i\varepsilon)\big)\\=&k\sum_{i=0}^{k-1}\big(C_k(x-i\varepsilon)-C_k(x-i\varepsilon-\varepsilon)\big)-\sum_{i=0}^{k-1}\big(C_k(x-i\varepsilon)-C_k(x-k\varepsilon-i\varepsilon)\big)\\=&(kI-A_{-k})\big(C_k(x)-C_k(x-k\varepsilon)\big).\end{aligned}$$

Using telescope sum trick again, we rewrite the right-hand side of (2.11) as

$$\begin{aligned}&\sum_{i=0}^{k-1}\big((k-1)C_{-k}(x-i\varepsilon)-kC_{-k}(x-i\varepsilon+\varepsilon)+C_{-k}(x-i\varepsilon+k\varepsilon)\big)\\=&k\sum_{i=0}^{k-1}\big(C_{-k}(x-i\varepsilon)-C_{-k}(x-i\varepsilon+\varepsilon)\big)+\sum_{i=0}^{k-1}\big(C_{-k}(x+(k-i)\varepsilon)-C_{-k}(x-k\varepsilon+(k-i)\varepsilon)\big)\\=&k\big(C_{-k}(x-k\varepsilon+\varepsilon)-C_{-k}(x+\varepsilon)\big)+\sum_{i=0}^{k-1}\big(C_{-k}(x+\varepsilon+i\varepsilon)-C_{-k}(x-k\varepsilon+\varepsilon+i\varepsilon)\big)\\=&T(kI-A_k)\big((C_{-k}(x-k\varepsilon)-C_{-k}(x)\big).\end{aligned}$$

Combining the above two identities, we rewrite (2.11) as

$$F(x)=F(x-k\varepsilon).$$

By iteration, there exists $i\in\mathbb{N}$ such that $F(x)=F(x-ik\varepsilon)=0$ with $x-ik\varepsilon\in\Omega_{\rm a}$. □

3 Consistency error estimate

In this part, we prove that the consistency error of GCS is first-order in an appropriate negative Sobolev norm. Let y be the solution of (1.5), the truncation error functional

$$\mathcal{F}[y]=\delta E_{\rm a}^{\rm tot}[y]-\delta E_{\rm gcs}^{\rm tot}[y]$$

can be decomposed according to the interaction ranges as

$$\mathcal{F}[y]=\sum_{k=1}^{r_{\rm cut}}\mathcal{F}_k(y)\quad\text{with}\ \ \mathcal{F}_k[y]=\delta E_{{\rm a},k}(y)-\delta E_{{\rm gcs},k}(y),$$

where $E_{{\rm a},k}(y)=\sum_{x\in\Omega_\varepsilon}\varepsilon\phi(D_ky(x))$. We start with the following representation of $\mathcal{F}_k[y]$.

Lemma 3.1. *Let y be the solution of* (1.5). *Then for any $k=1,\cdots,r_{cut}$ and $v\in\mathcal{U}_\varepsilon$,*

$$\begin{aligned}\langle\mathcal{F}_k[y],v\rangle=&\Big\langle A_{-k}\phi'(D_ky)-k\phi'(kDy),Dv\Big\rangle_{\Omega_{\rm c}}+\frac{1}{2}\big\langle A_{-k}\phi'(D_ky)-k\phi'(\mathcal{D}_ky),Dv\big\rangle_{\Omega_{\rm a/c}}\\&+\frac{1}{2}\big\langle A_{-k}\phi'(D_ky)-kT\phi'(-\mathcal{D}_{-k}y),Dv\big\rangle_{\Omega_{\rm a/c}}\\&+\frac{1}{2}\big\langle(kI-A_{-k})\big[C_k\phi'(\mathcal{D}_ky)\big]+T(kI-A_k)\big[C_{-k}\phi'(-\mathcal{D}_{-k}y)\big],Dv\big\rangle_{\Omega_{\rm a/c}}.\end{aligned}\tag{3.1}$$

The first term in the right-hand side of (3.1) is the so-called "model error", i.e., to what degree the atomistic model is approximated by the CB elastic model. The remaining three terms are the error committed by the GCS reconstruction, which are localized inside the a/c interface.

Proof. By (1.1), we have

$$\langle\delta E_{{\rm a},k}[y],v\rangle=\big\langle\phi'(D_ky),D_kv\big\rangle=\Big\langle A_{-k}\Big[\phi'(D_ky)\Big],Dv\Big\rangle.\tag{3.2}$$

Using (1.1) and (1.2), we obtain

$$\begin{aligned}\big\langle\phi'(\mathcal{D}_ky),\mathcal{D}_kv\big\rangle=&\sum_{x\in\Omega_{\varepsilon,k}}\phi'(\mathcal{D}_ky(x))\Big(C_k(x)D_kv(x)+k(1-C_k(x))Dv(x)\Big)\\=&\Big\langle A_{-k}\Big[C_k\phi'(\mathcal{D}_ky)\Big],Dv\Big\rangle+\big\langle k(1-C_k)\phi'(\mathcal{D}_ky),Dv\big\rangle,\end{aligned}$$

and

$$\begin{aligned}&-\big\langle\phi'(-\mathcal{D}_{-k}y),\mathcal{D}_{-k}v\big\rangle\\=&-\Big\langle A_k\Big[C_{-k}\phi'(-\mathcal{D}_{-k}y)\Big],D_-v\Big\rangle-\big\langle k(1-C_{-k})\phi'(-\mathcal{D}_{-k}y),D_-v\big\rangle\\=&\Big\langle T\Big[A_k\Big[C_{-k}\phi'(-\mathcal{D}_{-k}y)\Big]\Big],Dv\Big\rangle+\Big\langle T\Big[k(1-C_{-k})\phi'(-\mathcal{D}_{-k}y)\Big],Dv\Big\rangle.\end{aligned}$$

Combining the above two identities, we obtain

$$\begin{aligned}\big\langle\delta E_{{\rm gcs},k}(y),v\big\rangle=&\frac{1}{2}\big\langle A_{-k}[C_k\phi'(\mathcal{D}_ky)],Dv\big\rangle+\frac{1}{2}\big\langle k(1-C_k)\phi'(\mathcal{D}_ky),Dv\big\rangle\\&+\frac{1}{2}\Big\langle T\Big[k(1-C_{-k})\phi'(-\mathcal{D}_{-k}y)\Big],Dv\Big\rangle\\&+\frac{1}{2}\Big\langle T\Big[A_k\Big[C_{-k}\phi'(-\mathcal{D}_{-k}y)\Big]\Big],Dv\Big\rangle.\end{aligned}\tag{3.3}$$

It is clear that $\langle \delta E_{\mathrm{gcs},k}(y),v\rangle_{\Omega_{\mathrm{a}}}$ reduces to $\langle \delta E_{\mathrm{a},k}(y),v\rangle_{\Omega_{\mathrm{a}}}$, and $\langle \delta E_{\mathrm{gcs},k}(y),v\rangle_{\Omega_{\mathrm{c}}}$ changes to $\langle \delta E_{\mathrm{c},k}(y),v\rangle_{\Omega_{\mathrm{c}}}$. A combination of (3.2) and (3.3) yields (3.1). □

We denote the terms in the right-hand side of (3.1) by $I_1,\cdots,I_4$, respectively. It is by now well-known that the model error I_1 is of second-order (see e.g., [7] and [22]). I_2 and I_3 are of first-order because GCS is essentially a linear reconstruction scheme. I_4 may be bounded with the aid of the identity (2.10), which is also of first-order.

Lemma 3.2. *Let y be the solution of* (1.5)*, then for any $v\in\mathcal{U}_\varepsilon$,*

$$\begin{aligned}|\langle \mathcal{F}[y],v\rangle_{\Omega_\varepsilon}| \le & Cr_{cut}^3\varepsilon\|D^2y\|_{\ell_\varepsilon^{p'}(\widehat{\Omega}_{a/c})}\|Dv\|_{\ell_\varepsilon^p(\widehat{\Omega}_{a/c})}\\ &+Cr_{cut}^5\varepsilon^2\left(\|D^2y\|^2_{\ell_\varepsilon^{2p'}(\Omega_c)}+\|D^3y\|_{\ell_\varepsilon^{p'}(\Omega_c)}\right)\|Dv\|_{\ell_\varepsilon^p(\Omega_c)},\end{aligned}\tag{3.4}$$

where $\widehat{\Omega}_{a/c}=\Omega_{a/c}\pm r_{cut}\varepsilon$, $p'=p/(p-1)$, and C depends on $\|\phi^{(2)}\|_\infty$ and $\|\phi^{(3)}\|_\infty$.

If we assume that $\|D^jy\|_\infty$ is bounded for $j=2,3$, then

$$|\langle \mathcal{F}[y],v\rangle_{\Omega_\varepsilon}| \le Cr_{cut}^3\left(M_k^{1-1/p}\varepsilon^{2-1/p}\|Dv\|_{\ell_\varepsilon^p(\Omega_{a/c})}+r_{cut}^2\varepsilon^2\|Dv\|_{\ell_\varepsilon^p(\Omega_c)}\right).\tag{3.5}$$

According to [3], the above consistency result is essentially optimal.

Proof. By Taylor's expansion,

$$\begin{aligned}&A_{-k}\phi'(D_ky(x))-k\phi'(kDy(x))\\ =&\sum_{j=0}^{k-1}\phi''(\xi_{j,x})\big(D_ky(x-j\varepsilon)-kDy(x)\big)\\ =&\phi''(\xi_{0,x})\sum_{j=0}^{k-1}\big(D_ky(x-j\varepsilon)-kDy(x)\big)+\sum_{j=0}^{k-1}\big(\phi''(\xi_{j,x})-\phi''(\xi_{0,x})\big)\big(D_ky(x-j\varepsilon)-kDy(x)\big)\\ =&\phi''(\xi_{0,x})\sum_{j=0}^{k-1}\big(D_ky(x-j\varepsilon)-kDy(x)\big)+\varepsilon\sum_{j=0}^{k-1}\phi'''(\theta_{j,x})(\xi_{j,x}-\xi_{0,x})\sum_{l=0}^{k-1}D_{l-j}Dy(x),\end{aligned}$$

where $\xi_{j,x}\in\mathrm{conv}\,(D_ky(x-j\epsilon),kDy(x))$ and $\theta_{j,x}\in\mathrm{conv}(\xi_{j,x},\xi_{0,x})$. Here $\mathrm{conv}A$ denote the convex hull of a set $A\in\mathbb{R}$.

Next we write

$$\begin{aligned}&\sum_{j=0}^{k-1}(D_ky(x-j\varepsilon)-kDy(x))\\ =&\varepsilon\sum_{i,j=0}^{k-1}D_{i-j}Dy(x)=\varepsilon\sum_{i=1}^{k-1}(k-i)(D_i+D_{-i})Dy(x)\\ =&-\varepsilon^2\sum_{i=1}^{k-1}(k-i)D_iD_{-i}Dy(x),\end{aligned}$$

and for certain $s_j, s_0 \in (0,1)$, we write

$$\begin{aligned}\xi_{j,x}-\xi_{0,x} &= s_j(D_k y(x-j\varepsilon)-kDy(x))-s_0(D_k y(x)-kDy(x))\\ &= \varepsilon\left(s_j\sum_{i=0}^{k-1}D_{i-j}Dy(x)-s_0\sum_{i=0}^{k-1}D_iDy(x)\right).\end{aligned}$$

Combining all the above equations and using Höder's inequality, we obtain

$$|I_1| \le Ck^4\varepsilon^2\left(\|D^2y\|^2_{\ell_\varepsilon^{2p'}(\Omega_c)}+\|D^3y\|_{\ell_\varepsilon^{p'}(\Omega_c)}\right)\|Dv\|_{\ell_\varepsilon^p(\Omega_c)}.$$

For any $1 \le i \le k$, using

$$\begin{aligned}D_k y(x-i\varepsilon)-\mathcal{D}_k y(x) &= D_k\big(y(x-i\varepsilon)-y(x)\big)+(1-C_k(x))\big(D_k y(x)-kDy(x)\big)\\ &= \varepsilon D_k D_{-i}y(x)+\varepsilon\big(1-C_k(x)\big)\sum_{j=0}^{k-1}D_jDy(x),\end{aligned}$$

we obtain

$$|I_2| \le Ck^2\varepsilon\|D^2y\|_{\ell_\varepsilon^{p'}(\widehat{\Omega}_{a/c})}\|Dv\|_{\ell_\varepsilon^p(\Omega_{a/c})}.$$

Estimate I_3 is essentially the same with that of I_2. Using

$$D_k y(x-i\varepsilon)+\mathcal{D}_{-k}y(x+\epsilon) = \varepsilon D_k D_{k-i-1}y(x)+\varepsilon\big(1-C_{-k}(x+\varepsilon)\big)\sum_{j=0}^{k-1}D_{j+1-k}Dy(x),$$

we obtain

$$|I_3| \le Ck^2\varepsilon\|D^2y\|_{\ell_\varepsilon^{p'}(\widehat{\Omega}_{a/c})}\|Dv\|_{l_\varepsilon^p(\Omega_{a/c})}.$$

Using (2.10), we obtain

$$\begin{aligned}&(kI-A_{-k})\big[C_k\phi'(\mathcal{D}_k y)\big]+T(kI-A_k)\big[C_{-k}\phi'(-\mathcal{D}_{-k}y)\big]\\ &=(kI-A_{-k})\Big[C_k\big(\phi'(\mathcal{D}_k y)-\phi'(kDy)\big)\Big]+T(kI-A_k)\Big[C_{-k}\big(\phi'(-\mathcal{D}_{-k}y)-\phi'(kDy)\big)\Big].\end{aligned}$$

Note

$$\mathcal{D}_k y(x)-kDy(x) = \varepsilon C_k(x)\sum_{i=0}^{k-1}DD_i y(x),$$

we obtain

$$|I_4| \le Ck^2\varepsilon\|D^2y\|_{\ell_\varepsilon^{p'}(\Omega_{a/c})}\|Dv\|_{\ell_\varepsilon^p(\Omega_{a/c})}. \tag{3.6}$$

Summing up all the above estimates, we obtain (3.4).

By

$$\|D^j y\|_{\ell_\varepsilon^{p'}(\Omega_{a/c})} \le C\varepsilon^{1/p'}M_k^{1/p'}\|D^j y\|_{\ell_\varepsilon^\infty}, \quad j=2,3,$$

and (3.4), we obtain (3.5). □

4 Stability and convergence

In this part, we study the stability of GCS at the uniform state. There are a lot of work discussed the stability of 1d atomistic model as well as its QC approximation, we refer to [16, Section 7] for a review. Most of these results are restricted to second nearest neighborhood interaction except the following works. Li and Luskin [12] employed discrete Fourier transform to prove the sharp stability result for 1d atomistic model and its generalized QNL approximation with periodic boundary condition. Ortner, Shapeev and Zhang [21] proved the stability of an infinite chain, in particular, they proved the sharp stability of the reflection method. Discussions on the stability for atomic models with general interaction potentials and finite range interactions can be found in [7, 9, 11, 14] and the references therein, which are usually confined to periodic system.

Compared to the previous work, we study the stability of GCS for 1d atomic chain with Dirichlet boundary condition. Our analysis is in the same vein with [17]. The main ingredients are a generalized polarisation identity and a Wirtinger's type inequality. The new point is the key identity (2.10) for the reconstruction coefficients. We note that the suboptimal stability condition for GCS with second neighboring interaction in [17] is mainly due to a rough estimate of the "strain gradient" term $|D_2u|^2$.

4.1 Stability of atomistic and continuum model

A direct calculation gives

$$\left\langle \delta^2 E_a(y_F)v,v\right\rangle_{\Omega_\varepsilon}=\sum_{k=1}^{r_{\rm cut}}\phi''(kF)\|D_kv\|^2_{\ell^2_\varepsilon(\Omega_{\varepsilon,k})}. \tag{4.1}$$

By the hypothesis (1.3), we have

$$\phi''(kF)\le 0,\quad k\ge 2. \tag{4.2}$$

We firstly recall a discrete analogue of Wirtinger's inequality.

Lemma 4.1 (see [13]). *Suppose $v\in\mathcal{U}_\varepsilon$, there holds*

$$\lambda_k\varepsilon^{-2}\|v\|^2_{\ell^2_\varepsilon(\Omega_\varepsilon)}\le\|D_kv\|^2_{\ell^2_\varepsilon(\Omega_{\varepsilon,k})}\le\Lambda_k\varepsilon^{-2}\|v\|^2_{\ell^2_\varepsilon(\Omega_\varepsilon)},\qquad k\in\mathbb{N}, \tag{4.3}$$

where

$$\lambda_k=4\sin^2\frac{\pi}{2\lfloor N/k\rfloor+4}\quad\text{and}\quad\Lambda_k=4\cos^2\frac{\pi}{2\lfloor N/k\rfloor+4},$$

and $\lfloor x\rfloor$ denotes the greatest integer not exceeding x.

Lemma 4.2. *Under the assumption* (4.2)*, for any* $v\in\mathcal{U}_\varepsilon$*, there holds*

$$\left\langle \delta^2 E_{\mathrm{a}}[y_F]v,v\right\rangle \geq \lambda_{at}\|Dv\|_{\ell^2_\varepsilon}^2 \tag{4.4}$$

with

$$\lambda_{at}=\sum_{k=1}^{r_{cut}}\left(k^2-\sum_{i=1}^{k-1}(k-i)\lambda_i\right)\phi''(kF).$$

We may write λ_{at} as

$$\lambda_{\mathrm{at}}=\sum_{k=1}^{r_{\mathrm{cut}}}k^2\phi''(kF)-\sum_{k=2}^{r_{\mathrm{cut}}}\left(\sum_{i=1}^{k-1}(k-i)\lambda_i\right)\phi''(kF).$$

The first part of λ_{at} is the standard stability condition that has appeared in the previous work such as [12] and [8], while the second term represents the *finite size* effect, which disappears when one considers an infinite chain.

Proof. By Lagrange's identity, for $k\geq 2$, we obtain

$$\begin{aligned}|D_kv(x)|^2=&k\sum_{i=0}^{k-1}|Dv(x+i\varepsilon)|^2-\sum_{0\leq i<j\leq k-1}\big(Dv(x+i\varepsilon)-Dv(x+j\varepsilon)\big)^2\\=&k\sum_{i=0}^{k-1}|Dv(x+i\varepsilon)|^2-\varepsilon^2\sum_{i=1}^{k-1}\sum_{j=0}^{k-i-1}|D_iDv(x+j\varepsilon)|^2.\end{aligned}$$

Since $Dv(x)\equiv 0$ for $x\in\Omega_{\varepsilon,k}\setminus\Omega_{\varepsilon,1}$, we obtain

$$\sum_{x\in\Omega_{\varepsilon,k}}\varepsilon|Dv(x+i\varepsilon)|^2=\|Dv\|^2_{\ell^2_\varepsilon(\Omega_{\varepsilon,1})},\quad i=0,\cdots,k-1.$$

For $i=1,\cdots,k-1$ and $j=0,\cdots,k-i-1$, there holds

$$\sum_{x\in\Omega_{\varepsilon,k}}|D_iDv(x+j\varepsilon)|^2=\sum_{x\in\Omega_{\varepsilon,i+1}}|D_iDv(x)|^2.$$

Combining the above identities, we obtain

$$\|D_kv\|^2_{\ell^2_\varepsilon}=k^2\|Dv\|^2_{\ell^2_\varepsilon}-\sum_{i=1}^{k-1}(k-i)\varepsilon^2\|D_iDv\|^2_{\ell^2_\varepsilon(\Omega_{\varepsilon,i+1})},$$

which together with the Wirtinger's inequality (4.3) yields

$$\|D_kv\|^2_{\ell^2_\varepsilon}\leq\left(k^2-\sum_{i=1}^{k-1}(k-i)\lambda_i\right)\|Dv\|^2_{\ell^2_\varepsilon(\Omega_{\varepsilon,1})}.$$

A combination of (4.1), (4.2) and the above inequality gives (4.4). □

Remark 4.1. Let

$$w(i\varepsilon)=\begin{cases}\varepsilon\big(-1+\cos(N+i+1)\theta\big), & i=-N,\cdots,N,\\ 0, & \text{others},\end{cases}$$

where $\theta=\pi/(N+1)$, and it is clear that $w\in\mathcal{U}_\varepsilon$. A direct calculation yields

$$\|D_k w\|_{\ell^2_\varepsilon}^2=4\varepsilon\sin^2(k\theta/2)\sum_{j=1}^{2N+1}\cos^2 j\theta+2\varepsilon\sum_{j=1}^{k}(1-\cos j\theta)(1-\cos(j-k)\theta).$$

In particular,

$$\|Dw\|_{\ell^2_\varepsilon}^2=4\varepsilon\sin^2(\theta/2)\sum_{j=1}^{2N+1}\cos^2(j\theta).$$

By the above identities, we obtain

$$\|D_k w\|_{\ell^2_\varepsilon}^2\geq\left(\sin\frac{k\theta}{2}\Big/\sin\frac{\theta}{2}\right)^2\|Dw\|_{\ell^2_\varepsilon}^2.$$

By (4.1), (4.2) and the above inequality, we conclude

$$\big\langle\delta^2E_{\rm a}[y_F]w,w\big\rangle\leq\Lambda_{\rm at}\|Dw\|_{\ell^2_\varepsilon}^2$$

with

$$\Lambda_{\rm at}=\sum_{k=1}^{r_{\rm cut}}(\sin(k\theta)/\sin\theta)^2\phi''(kF).$$

The difference between $\lambda_{\rm at}$ and $\Lambda_{\rm at}$ is of $\mathcal{O}(\varepsilon^2)$. Therefore, the stability condition of the atomistic model is sharp.

4.2 Stability of the geometrically consistent scheme

The stability of GCS with finite range interaction is as follows.

Theorem 4.1. *If we assume* $0\leq C_{\pm k}(x)\leq 1$ *for* $x\in\Omega_\varepsilon$ *and* (4.2) *is valid, then*

$$\big\langle\delta^2E_{a/c}[y_F]v,v\big\rangle\geq\lambda_{gcs}\|Dv\|_{\ell^2_\varepsilon}^2\quad\text{for any }\ v\in\mathcal{U}_\varepsilon,\tag{4.5}$$

where $\lambda_{gcs}=\sum_{k=1}^{r_{cut}}k^2\phi''(kF)$.

This theorem extends the stability result in [17] to system with finite range interaction. The stability condition is sharper than that in [17] when $r_{\rm cut}=2$. This stability condition is sharp in the sense that the difference between $\lambda_{\rm gcs}$ and $\lambda_{\rm at}$ is of $\mathcal{O}(\varepsilon^2)$.

Proof. For any $v\in\mathcal{U}_\varepsilon$, a direct calculation gives

$$\langle \delta^2 E_{\rm gcs}[y_F]v,v\rangle = \frac{1}{2}\sum_{k=1}^{r_{\rm cut}}\phi''(kF)\big(\langle \mathcal{D}_k v,\mathcal{D}_k v\rangle + \langle \mathcal{D}_{-k}v,\mathcal{D}_{-k}v\rangle\big). \tag{4.6}$$

By Lagrange's identity, we obtain

$$\begin{aligned}\sum_{x\in\Omega_{\varepsilon,k}} C_k^2(x)|D_k v(x)|^2 =& k\sum_{x\in\Omega_{\varepsilon,k}} C_k^2(x)\sum_{i=0}^{k-1}|Dv(x+i\varepsilon)|^2\\ &-\sum_{x\in\Omega_{\varepsilon,k}} C_k^2(x)\sum_{0\le i<j\le k-1}\big(Dv(x+i\varepsilon)-Dv(x+j\varepsilon)\big)^2.\end{aligned}$$

Noting that $D_k v(x)=\sum_{i=0}^{k-1}Dv(x+i\varepsilon)$ and using the basic identity $2ab=a^2+b^2-(a-b)^2$ for $a,b\in\mathbb{R}$, we obtain

$$\begin{aligned}&2k\sum_{x\in\Omega_{\varepsilon,k}} C_k(x)(1-C_k(x))D_k v(x)Dv(x)\\ =&k^2\sum_{x\in\Omega_{\varepsilon,k}} C_k(x)(1-C_k(x))|Dv(x)|^2\\ &+k\sum_{x\in\Omega_{\varepsilon,k}} C_k(x)(1-C_k(x))\sum_{i=0}^{k-1}\big(|Dv(x+i\varepsilon)|^2-|Dv(x+i\varepsilon)-Dv(x)|^2\big).\end{aligned}$$

By the above two identities and note

$$\sum_{x\in\Omega_{\varepsilon,k}} C_k(x)\sum_{i=0}^{k-1}|Dv(x+i\varepsilon)|^2=\sum_{x\in\Omega_{\varepsilon,1}}|Dv(x)|^2A_{-k}C_k(x),$$

we obtain

$$\begin{aligned}\langle \mathcal{D}_k v,\mathcal{D}_k v\rangle =& k^2\sum_{x\in\Omega_{\varepsilon,1}}|Dv(x)|^2+k\sum_{x\in\Omega_{\varepsilon,1}}|Dv(x)|^2(A_{-k}-kI)C_k(x)\\ &-\sum_{x\in\Omega_{\varepsilon,k}} C_k^2(x)\sum_{0\le i<j\le k-1}|Dv(x+i\varepsilon)-Dv(x+j\varepsilon)|^2\\ &-k\sum_{x\in\Omega_{\varepsilon,k}} C_k(x)(1-C_k(x))\sum_{i=0}^{k-1}|Dv(x+i\varepsilon)-Dv(x)|^2.\end{aligned}\tag{4.7}$$

Proceeding the same line that leads to (4.7), and using the fact that

$$\|Dv\|_{\ell^2_\varepsilon(\Omega_{\varepsilon,1})}=\|D_- v\|_{\ell^2_\varepsilon(\Omega_{\varepsilon,-1})},$$

we obtain

$$\begin{aligned}\langle \mathcal{D}_{-k}v,\mathcal{D}_{-k}v\rangle =& k^2\sum_{x\in\Omega_{\varepsilon,1}}|Dv(x)|^2+k\sum_{x\in\Omega_{\varepsilon,1}}|Dv(x)|^2T(A_k-kI)C_{-k}(x)\\ &-\sum_{x\in\Omega_{\varepsilon,-k}}C_{-k}^2(x)\sum_{1\le i<j\le k}\big(Dv(x-i\varepsilon)-Dv(x-j\varepsilon)\big)^2\\ &-\sum_{x\in\Omega_{\varepsilon,-k}}C_{-k}(x)(1-C_{-k}(x))\sum_{i=1}^{k}\big(Dv(x-i\varepsilon)-Dv(x-\varepsilon)\big)^2.\end{aligned}$$

Adding up $\langle \mathcal{D}_k v,\mathcal{D}_k v\rangle+\langle \mathcal{D}_{-k}v,\mathcal{D}_{-k}v\rangle$, and noting the second term vanishes by (2.10), we obtain, for $k\ge 2$,

$$\begin{aligned}&\langle \mathcal{D}_k v,\mathcal{D}_k v\rangle+\langle \mathcal{D}_{-k}v,\mathcal{D}_{-k}v\rangle\\ =&2k^2\|Dv\|_{\ell_\varepsilon^2}^2-\sum_{x\in\Omega_{\varepsilon,k}}C_k^2(x)\sum_{0\le i<j\le k-1}\big(Dv(x+i\varepsilon)-Dv(x+j\varepsilon)\big)^2\\ &-k\sum_{x\in\Omega_{\varepsilon,k}}C_k(x)(1-C_k(x))\sum_{i=0}^{k-1}\big(Dv(x+i\varepsilon)-Dv(x)\big)^2\\ &-\sum_{x\in\Omega_{\varepsilon,-k}}C_{-k}^2(x)\sum_{1\le i<j\le k}\big(Dv(x-i\varepsilon)-Dv(x-j\varepsilon)\big)^2\\ &-k\sum_{x\in\Omega_{\varepsilon,-k}}C_{-k}(x)(1-C_{-k}(x))\sum_{i=1}^{k}\big(Dv(x-i\varepsilon)-Dv(x-\varepsilon)\big)^2,\end{aligned}\tag{4.8}$$

which together with (4.6) immediately implies

$$\big\langle \delta^2E_{\rm gcs}[y_F]v,v\big\rangle\ge\left(\sum_{k=1}^{r_{\rm cut}}k^2\phi''(kF)\right)\|Dv\|_{\ell_\varepsilon^2}^2,$$

where we have used the assumption $0\le C_{\pm k}(x)\le 1$. □

Based on the consistency error estimate and stability result, following essentially the same line of [17] with minor modification, we obtain the following convergence result and error estimate for GCS with finite range interaction.

Theorem 4.2. *Assume that the condition* (4.2) *and the geometrically consistent condition* (1.11) *hold. There exists a constant* κ_1 *such that if* $\|f\|_{W^{m,p}(\Omega)}\le\kappa_1$ *for* $p\ge 1$ *and* $m\ge 4$, *then Problem* (1.9) *has a locally unique solution* y_{gcs} *such that*

$$\begin{aligned}\|D(y_{\rm a}-y_{gcs})\|_{\ell_\varepsilon^p}\le& Cr_{cut}^3\varepsilon^{2/p}\|D^2y_{\rm a}\|_{\ell_\varepsilon^{p'}(\widehat{\Omega}_{\rm a/c})}\\ &+Cr_{cut}^5\varepsilon^{1+2/p}\Big(\|D^2y_{\rm a}\|^2_{\ell_\varepsilon^{2p'}(\Omega_{\rm c})}+\|D^3y_{\rm a}\|_{\ell_\varepsilon^{p'}(\Omega_{\rm c})}\Big),\end{aligned}\tag{4.9}$$

where $2\le p\le\infty, p'=p/(p-1)$ *and* C *depends on* $\|\phi^{(2)}\|_\infty$ *and* $\|\phi^{(3)}\|_\infty$.

If $D^k y_{\rm a}$ *is uniformly bounded for* $k=2,3$, *then*

$$\|D(y_{\rm a}-y_{gcs})\|_{\ell^p_\varepsilon}\le C\varepsilon^{1+1/p},\quad 2\le p\le\infty. \tag{4.10}$$

5 Numerical results

In this part, we report the performance of GCS through a set of representative numerical examples. We consider a 1d chain interacted with the Morse potential [18]

$$\varphi(r)=\exp\big(2\alpha(r-1)\big)-2\exp\big(\alpha(r-1)\big),$$

where α is a parameter related to the decay behavior of the potential function. We test both the smooth and the non-smooth external forces. The former is covered by our theoretical results, while the latter is escaped from our theoretical results.

In each example, we report the results for $\|D(y_{\rm a}-y_{\rm gcs})\|_{\ell^p_\varepsilon}$ with $p=2,4,8,\infty$ and $r_{\rm cut}=4,10$. We shall also compare the accuracy of GCS with different reconstruction coefficients.

5.1 Smooth external force

We let $\Omega_{\rm a}=[1,1/4]\cup[3/4,1]$ and $\Omega_{\rm c}=(1/4,3/4)$, and assume

$$f(x)=\sin(2\pi x)$$

and

$$\alpha=1.95.$$

We use GCS coefficients (2.6) in the simulation, and plot the error with different $r_{\rm cut}$ in Fig. 1 and Fig. 2. It is clear that the convergence rate is $\mathcal{O}(\varepsilon^{1+1/p})$ as predicted by (4.10).

Next we test the influence of the GCS coefficients. We use the ℓ^2-minimizer (2.8) as GCS coefficients, and plot the error with different $r_{\rm cut}$ in Fig. 3 and Fig. 4. The results with ℓ^1-minimizer as GCS coefficients were reported in Fig. 5 and Fig. 6.

By the results in Fig. 1 to Fig. 6, we found that both the error with ℓ^1-minimizer GCS coefficient and ℓ^2-minimizer GCS coefficient are slightly smaller than those of (2.6) and (2.7). We wonder this is due to the fact that the former has a smaller consistency error. It is worthwhile to mention that we have not observed the numerical instability caused by the ℓ^2-minimizer GCS coefficient as reported in [25]. This may be due to the fact that the minimizing problem for GCS has much smaller size compared to the method in [25]. We shall pursue this issue in further study.

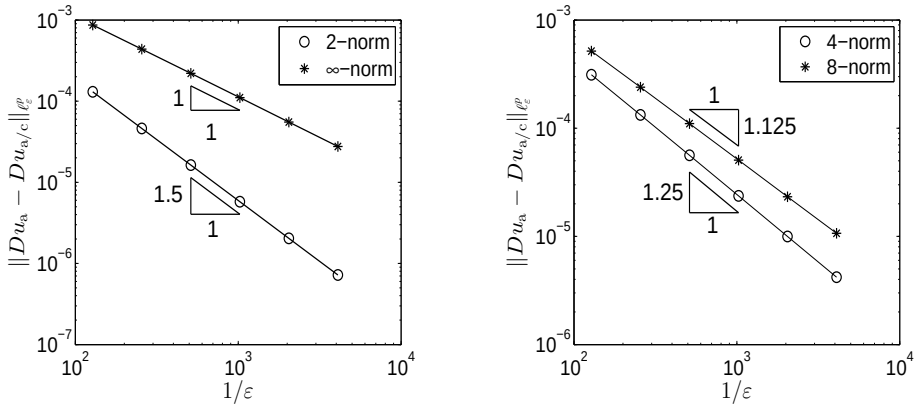

(a) (b)

Figure 1: Plots of $\|D(y_a - y_{gcs})\|_{\ell^p_\varepsilon}$ with $p=2,4,8,\infty$, for the Morse potential with $\alpha=1.95$ and $r_{cut}=4$. GCS coefficients are taken from (2.6).

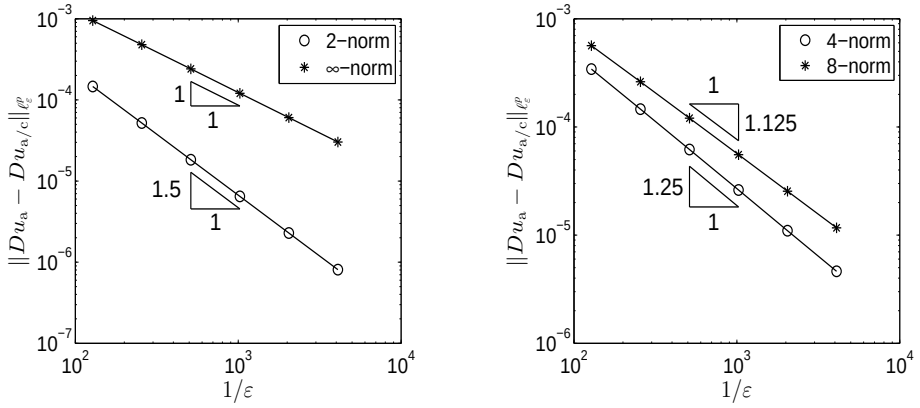

(a) (b)

Figure 2: Plots of $\|D(y_a - y_{gcs})\|_{\ell^p_\varepsilon}$ with $p=2,4,8,\infty$, for the Morse potential with $\alpha=1.95$ and $r_{cut}=10$. GCS coefficients are taken from (2.6).

5.2 Non-smooth external forces

For many 2D/3D crystal materials, a vacancy or interstitial atom will cause a rapidly decaying deformation. As [23], we impose on a discrete delta force

$$f_n = \begin{cases} -128, & n = N/2, \\ 12, & n = N/2+1, \\ 0, & \text{otherwise}, \end{cases}$$

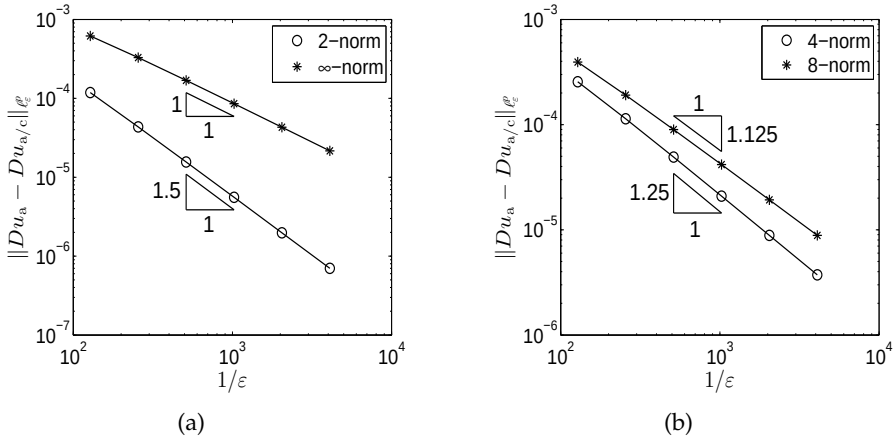

Figure 3: Plots of $\|D(y_a - y_{gcs})\|_{\ell^p_\varepsilon}$ with $p = 2,4,8,\infty$, for the Morse potential with $\alpha = 1.95$ and $r_{cut} = 4$. ℓ^2-minimizer is used for GCS coefficients.

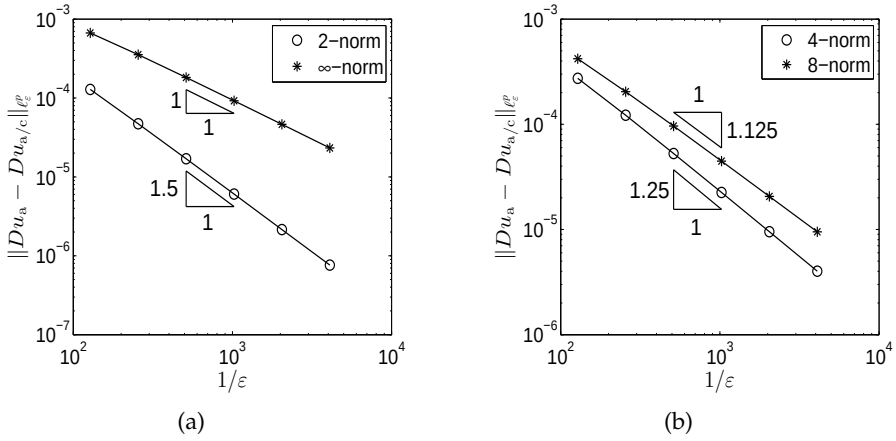

Figure 4: Plots of $\|D(y_a - y_{gcs})\|_{\ell^p_\varepsilon}$ with $p = 2,4,8,\infty$, for the Morse potential with $\alpha = 1.95$ and $r_{cut} = 10$. ℓ^2-minimizer is used for GCS coefficients.

where the number of the atoms is $N = 256$. The above force draw apart the atoms $n = 128$ and $n = 129$, creating a non-smooth perturbation of displacement. By Fig. 7(a), it is clear that the displacement gradient is large near the atom $n = 128$, but decays rapidly to a very small uniform deformation.

In the simulation we use the Morse potential with $\alpha = 2.4$. We let $r_{cut} = 4$, and $\Omega_a = \{108,\cdots,149\}$, $\Omega_c = \{1,\cdots,101\}\cup\{156,\cdots,256\}$, and $\Omega_{a/c} = \{102,\cdots,107\}\cup\{150,\cdots,155\}$. The GCS coefficients (2.6) and (2.7) are used in $\Omega_{a/c}$. We denote by y_{qc} the solution of the original QC method. Fig. 7$_b$ shows that D^2u_a decay rapidly to zeros from the center atoms $n = 128$ and $n = 129$. We plot the error of displacement gradient in Fig. 8. The

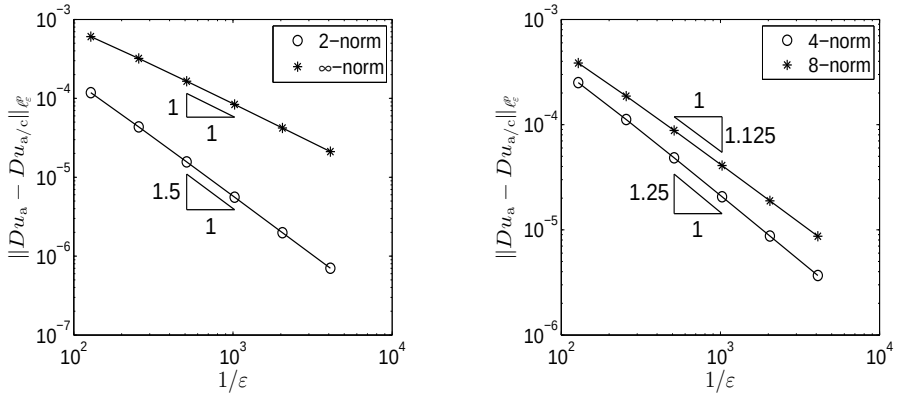

(a) (b)

Figure 5: Plots of $\|D(y_a - y_{gcs})\|_{\ell^p_\varepsilon}$ with $p = 2,4,8,\infty$, for the Morse potential with $\alpha = 1.95$ and $r_{cut} = 4$. ℓ^1-minimizer is used for GCS coefficients.

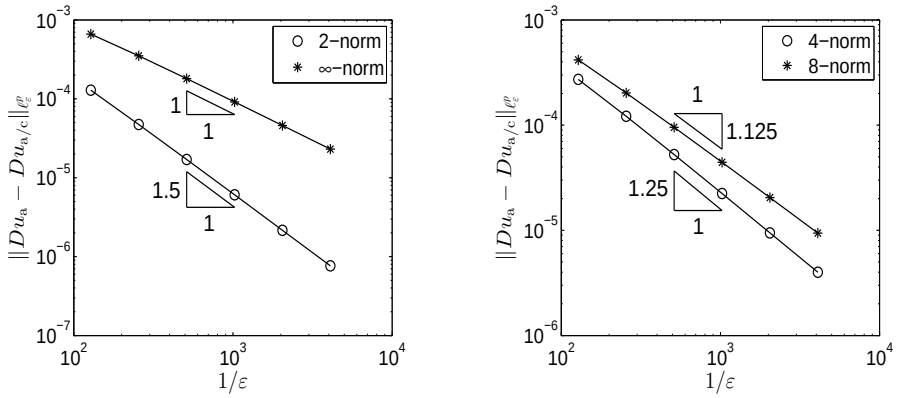

(a) (b)

Figure 6: Plots of $\|D(y_a - y_{gcs})\|_{\ell^p_\varepsilon}$ with $p = 2,4,8,\infty$, for the Morse potential with $\alpha = 1.95$ and $r_{cut} = 10$. ℓ^1-minimizer is used for GCS coefficients.

QC method has a large error in the interfacial regions, while GCS achieves a machine accuracy.

For many real defects in 2D/3D crystal materials, the decay of the strain is fairly slow due to the presence of defect. Similar to [23], we define the external force as

$$f_n = \begin{cases} 0.2\left(\cos\dfrac{2(n-1)\pi}{N} - 1\right), & 1 \le n \le (N+1)/2, \\ 0.2\left(\cos\dfrac{(2n-N-2)\pi}{N} + 1\right), & (N+3)/2 \le n \le N, \end{cases}$$

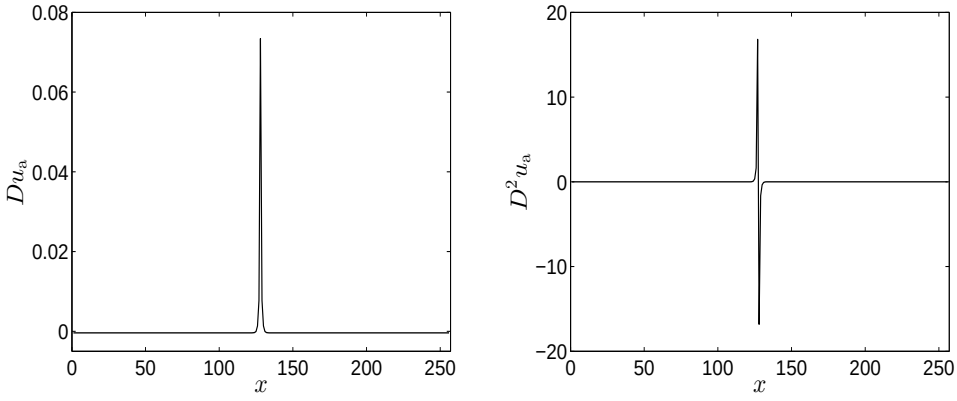

(a) (b)

Figure 7: Plots of Du_a and D^2u_a for the atomistic model

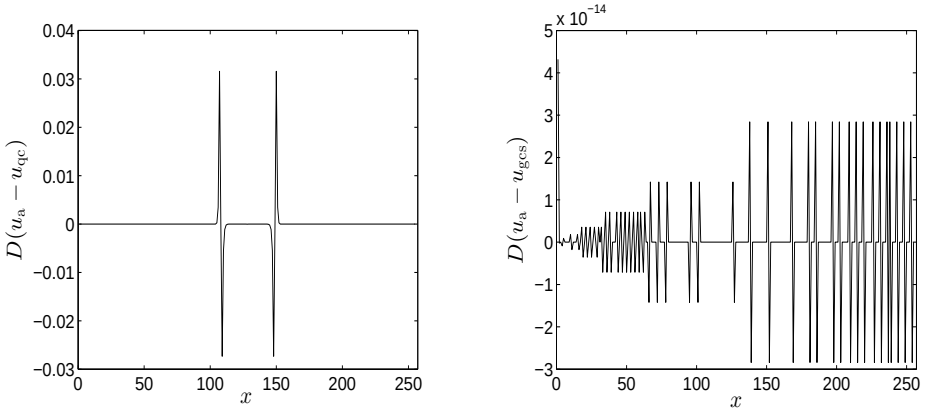

(a) (b)

Figure 8: Plots of pointwise error $D(u_a - u_{qc})$ and $D(u_a - u_{gcs})$.

where the number of the atoms is $N = 257$.

We assume $\alpha = 2.4$ and $r_{cut} = 4$, and $\Omega_a = \{67,\cdots,187\}$, $\Omega_c = \{1,\cdots,60\} \cup \{194,\cdots,257\}$, and $\Omega_{a/c} = \{61,\cdots,66\} \cup \{188,\cdots,193\}$. The GCS coefficients (2.6) and (2.7) are used in the simulation. Fig. 9 shows that the displacement gradient Du_a is nowhere locally uniform, and D^2u_a decay slowly away from the center. We plot the displacement gradient error for QC and GCS in Fig. 10. Both methods have relatively large error in the interfacial region, while the error in GCS is much smaller than that of QC. Such error is caused by the slow decay behavior of D^2u_a, and the term $r_{cut}^3 \varepsilon^{2/p} \|D^2 y_a\|_{\ell_\varepsilon^{p'}(\widehat{\Omega}_{a/c})}$ dominates in the error estimate (4.9). Such error is negligible when D^2u_a is close to zero in the interfacial regions; see Fig. 7.

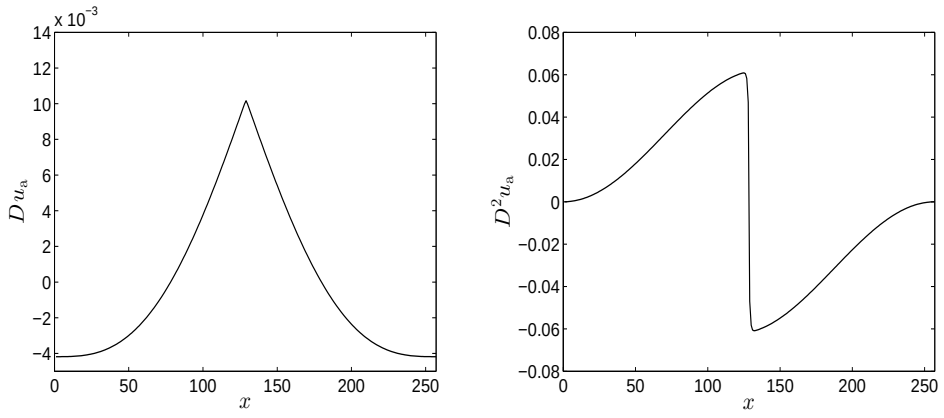

Figure 9: Plots of Du_a and D^2u_a for atomistic model

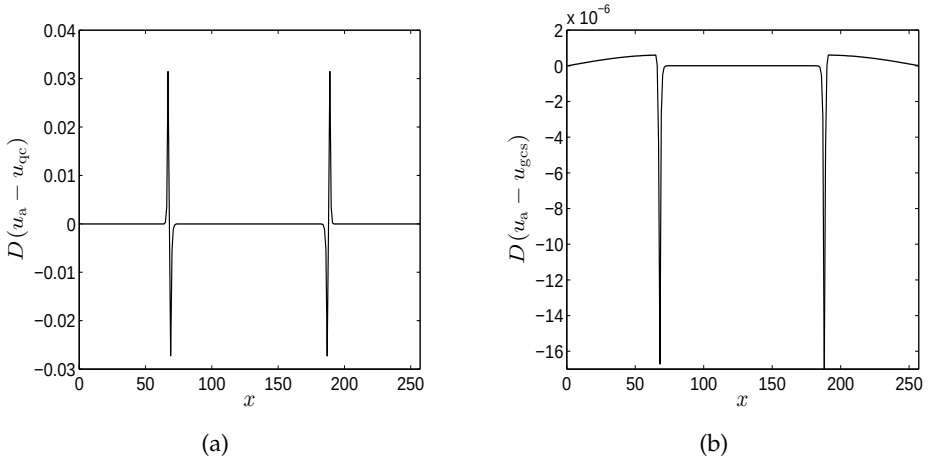

Figure 10: Plots of pointwise error $D(u_a - u_{qc})$ and $D(u_a - u_{gcs})$.

5.3 Tensile atomistic chain

Consider a finite chain, where the number of atoms is $N = 203$ and the atoms are labeled from $x = -101$ to $x = 101$. The atoms $x = -101$ and $x = 101$ are fixed, and other atoms are free to deform. We consider the Morse interaction with $\alpha = 2$ and $r_{cut} = 4$. We tensile the atoms $x = -101$ and $x = 101$ oppositely until the macroscopic strain reaches $\varepsilon = 0.01$. To resolve the relaxation near the boundary, we assume that $\Omega_a = \{\pm 100, \cdots, \pm 85\}$, $\Omega_c = \{-78, \cdots, 78\}$, and $\Omega_{a/c} = \{\pm 79, \cdots, \pm 84\}$, where the thickness of the buffer layer is 6. The GCS coefficients (2.6) and (2.7) are used in the simulation. Fig. 11 shows the pointwise relative error of strain for the CB elastic model, the original QC method and GCS.

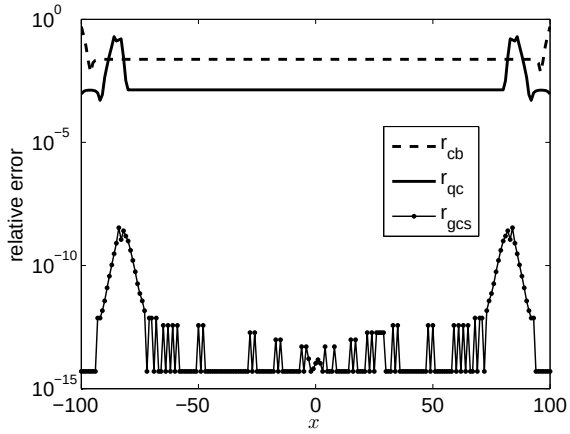

Figure 11: Plots of pointwise relative error of strain.

Nearly fifty percent error around the boundary was observed for the CB elastic model, while the relative error away from the boundary is rather small. The QC method resolves relaxation, while it has nearly twenty percent error near the a/c interface. GCS almost approaches to the machine precision. This example is consistent with our theoretical prediction.

Appendix: Auxiliary results for the reconstruction coefficients

The following tables list certain auxiliary results for the GCS reconstruction coefficients for the minimizing problems (2.8) and (2.9).

Table 4: The ℓ^1 optimal GCS coefficient $C_k(x)$.

	ε	2ε	3ε	4ε	5ε	6ε	7ε	8ε	9ε
$C_2(x)$	0	0	0	0	0	0	0	0	0
$C_3(x)$	0.5202	-0.2292	0.1006	-0.0431	0.0177	-0.0070	0	0	0
$C_4(x)$	0.6667	0.2222	-0.3889	0.1667	0	0	0	0	0
$C_5(x)$	0.7847	0.4694	0.0541	-0.4612	0	0	0	0	0

Table 5: The ℓ^1 optimal GCS coefficient $C_{-k}(x)$.

	ε	2ε	3ε	4ε	5ε	6ε	7ε	8ε	9ε
$C_{-2}(x)$	1	1	0	0	0	0	0	0	0
$C_{-3}(x)$	1	1	1	0.0404	-0.0190	0.0100	-0.0057	0.0036	-0.0035
$C_{-4}(x)$	1	1	1	1	0	0	-0.0556	0.0556	0
$C_{-5}(x)$	1	1	1	1	1	0.1388	-0.0459	-0.1306	-0.1153

Table 6: The ℓ^2 optimal GCS coefficient $C_k(x)$.

	ε	2ε	3ε	4ε	5ε	6ε	7ε	8ε	9ε
$C_2(x)$	0	0	0	0	0	0	0	0	0
$C_3(x)$	0.5001	-0.2500	0.1250	-0.0625	0.0313	-0.0156	0	0	0
$C_4(x)$	0.6697	0.2288	-0.3756	0.1742	0.0091	0	0	0	0
$C_5(x)$	0.7833	0.4667	0.0500	-0.4667	0	0	0	0	0

Table 7: The ℓ^2 optimal GCS coefficient $C_{-k}(x)$.

	ε	2ε	3ε	4ε	5ε	6ε	7ε	8ε	9ε
$C_{-2}(x)$	1	1	0	0	0	0	0	0	0
$C_{-3}(x)$	1	1	1	2.44e-4	-4.88e-4	9.77e-4	-0.0020	0.0039	-0.0078
$C_{-4}(x)$	1	1	1	1	0.0091	0.0076	-0.0424	0.0621	0.0030
$C_{-5}(x)$	1	1	1	1	1	0.1333	-0.0500	-0.133	-0.1167

Table 8: The ℓ^2 optimal GCS coefficient $C_k(x)$ with positive constraint.

	ε	2ε	3ε	4ε	5ε	6ε	7ε	8ε	9ε
$C_2(x)$	4.58e-4	4.58e-4	4.58e-4	4.58e-4	4.58e-4	4.58e-4	4.58e-4	0	0
$C_3(x)$	0.6251	3.77e-15	0.1563	1.51e-14	0.0391	1.15e-15	0	0	0
$C_4(x)$	0.7845	0.4689	3.75e-12	0.2264	0.0404	0	0	0	0
$C_5(x)$	0.9000	0.7000	0.4000	2.55e-21	0	0	0	0	0

Table 9: The ℓ^2 optimal GCS coefficient $C_{-k}(x)$ with positive constraint.

	ε	2ε	3ε	4ε	5ε	6ε	7ε	8ε	9ε
$C_{-2}(x)$	1	1	4.58e-4	4.58e-4	4.58e-4	4.58e-4	4.58e-4	4.58e-4	4.58e-4
$C_{-3}(x)$	1	1	1	0.2503	0.1245	0.0635	0.0293	0.0195	5.77e-16
$C_{-4}(x)$	1	1	1	1	0.3535	0.2685	0.1246	0.0934	0.0135
$C_{-5}(x)$	1	1	1	1	1	0.6000	0.3000	0.1000	1.21e-16

Acknowledgments

The work of Li was supported by Science Challenge Project, TZ 2016003. The work of Ming was partially supported by the National Natural Science Foundation of China for Distinguished Young Scholars 11425106, and National Natural Science Foundation of China grants 91630313, and by the support of CAS NCMIS.

References

[1] S. Badia, M. L. Parks, M. Gunzburger, P. B. Bochev, and R. B. Lehoucq, On atomistic-to-continuum coupling by blending, Multiscale Model. Simul., 7 (2008), 381–406.
[2] M. Born and K. Huang, Dynamical Theory of Crystal Lattices, Oxford University Press, 1954.
[3] M. Dobson, There is no pointwise consistent quasicontinuum energy, IMA J. Numer. Anal., 279 (2014), 29–45.
[4] M. Dobson and M. Luskin, An analysis of the effect of ghost force oscillation on quasicontinuum error, ESAIM: M2AN, 43 (2009), 591–604.
[5] W. E, Principles of Multiscale Modeling, Cambridge University Press, 2011.
[6] W. E, J. Lu, and J. Z. Yang, Uniform accuracy of the quasicontinuum method, Phys. Rev. B, 74 (2006), 214115.
[7] W. E and P. B. Ming, Cauchy-Born rule and the stability of crystalline solids: static problems, Arch. Ration. Mech. Anal., 183 (2007), 241–297.
[8] B. Houchmandzadeh, J. Lajzerowicz, and E. Salje, Relaxations near surfaces and interfaces for first-, second- and third-neighbour interactions: theory and applications to polytypism, J. Phys. Condens. Matter, 4 (1992), 9779–9794.
[9] T. Hudson and C. Ortner, On the stability of Bravais lattices and their Cauchy-Born approximations, ESAIM: M2AN, 46 (2012), 81–110.
[10] J. E. Lennard-Jones, On the force between atoms and ions, Proc. R. Soc. London Ser. A, 109 (1925), 584–597.
[11] X. H. Li and M. Luskin, Lattice stability for atomistic chains modeled by local approximations of the embedded atom method, Comput. Mater. Sci., 66 (2013), 96–103.
[12] X. H. Li and M. Luskin, A generalized quasinonlocal atomistic-to-continuum coupling method with finite-range interaction, IMA J. Numer. Anal., 32 (2012), 373–393.
[13] László Losonczi, On some discrete quadratic inequalities, Int. Ser. Numer. Math., 80 (1987), 73–85.
[14] J. Lu and P. B. Ming, Convergence of a force-based hybrid method in three dimensions, Commun. Pure Appl. Math., 66 (2013), 83–108.
[15] Jianfeng Lu and Pingbing Ming, Stability of a force-based hybrid method in three dimension with sharp interface, SIAM J. Numer. Anal., 52 (2014), 2005–2026.
[16] M. Luskin and C. Ortner, Atomistic-to-continuum coupling, Acta Numer., (2013), 397–508.
[17] P. B. Ming and J. Z. Yang, Analysis of a one-dimensional nonlocal quasicontinuum method, Multiscale Model. Simul., 7 (2009), 1838–1875.
[18] P. M. Morse, Diatomic molecules according to the wave mechanics, II, Viberational levels, Phys. Rev., 34 (1929), 57–64.
[19] D. Olson, P. B. Bochev, M. Luskin, and A. V. Shapeev, An optimization-based atomistic-to-continuum coupling method, SIAM J. Numer. Anal., 52 (2014), 2183–2204.
[20] C. Ortner, A priori and a posteriori analysis of the quasinonlocal quasicontinuum method in 1D, Math. Comput., 80 (2011), 1265–1285.
[21] C. Ortner, A. Shapeev, and L. Zhang, (in-)stability and stabilization of QNL-type atomistic-to-continuum coupling methods, Multiscale Model. Simul., 12 (2014), 1258–1293.
[22] C. Ortner and F. Theil, Justification of the Cauchy-Born approximation of elastodynamics, Arch. Rational Mech. Anal., 207 (2013), 1025–1073.
[23] C. Ortner and H. Wang, A priori error estimates for energy-based quasicontinuum approximations of a periodic chain, Math. Models Methods Appl. Sci., 21 (2011), 2491–2521.
[24] C. Ortner and L. Zhang, Construction and sharp consistency estimates for atom-

istic/continuum coupling methods with general interfaces: a two-dimensional model problems, SIAM J. Numer. Anal., 50 (2012), 2940–2965.
[25] C. Ortner and L. Zhang, Energy-based atomictic-to-continuum coupling without ghost forces, Comput. Methods Appl. Mech. Eng., 279 (2014), 29–45.
[26] M. L. Parks, P. B. Bochev, and R. B. Lehoucq, Connecting atomistic-to-continuum coupling and domain decompositiong, Multiscale Model. Simul., 7 (2008), 362–380.
[27] A. V. Shapeev, Consistent energy-based atomistic/continuum coupling for two-body potentials in one and two dimension, Multiscale Model. Simul., 9 (2011), 905–932.
[28] Alexander V. Shapeev, Consistent energy-based atomistic/continuum for two-body potential in three dimensions, SIAM J. Sci. Comput., 34(3) (2012), B335–B360.
[29] V. B. Shenoy, R. Miller, E. B. Tadmor, D. Rodney, R. Phillips, and M. Ortiz, An adaptive finite element approach to atomic-scale mechanics-the quasicontinuum method, J. Mech. Phys. Solids, 47 (1999), 611–642.
[30] T. Shimokawa, J. J. Mortensen, J. Schiøtz, and K. W. Jacobsen, Matching conditions in the quasicontinuum method: Removal of the error introduced at the interface between the coarse-grained and fully atomistic region, Phys. Rev. B, 69 (2004), 214104.
[31] E. B. Tadmor, M. Ortiz, and R. Phillips, Quasicontinuum analysis of defects in solids, Philos. Mag. A, 73 (1996), 1529–1563.
[32] B. Van Koten and M. Luskin, Analysis of energy-based bnended quasi-continuum approximations, SIAM J. Numer. Anal., 49 (2011), 2182–2209.